Hindawi
Geofluids
Volume 2022, Article ID 9073442, 10 pages
https://doi.org/10.1155/2022/9073442

Research Article

The Numerical Stimulation of Methane-Air Mixing Characteristics in Wellbore during the Air Jet Injection

Zhixiang Tao,[1,2] **Chengzheng Cai**,[1,2] **Zengxin Zou**,[1,2] **Yugui Yang**,[1,2] **and Yinrong Feng**[1,2]

[1]*State Key Laboratory for Geomechanics and Deep Underground Engineering, China University of Mining and Technology, Xuzhou 221116, China*
[2]*School of Mechanics and Civil Engineering, China University of Mining and Technology, Xuzhou 221116, China*

Correspondence should be addressed to Chengzheng Cai; caicz@cumt.edu.cn

Received 8 April 2022; Revised 18 May 2022; Accepted 21 May 2022; Published 6 June 2022

Academic Editor: Hasan N. Al-Saedi

At present, in situ blasting fracturing with formation methane is identified as an effective method for shale gas stimulation. In this paper, based on the in situ temperature and pressure conditions, a horizontal wellbore model filled with methane was established to simulate the methane-air mixing characteristics in wellbore during air jet. According to the distributions of the methane concentration and flow field characteristics, methane-air mixing inside the wellbore can be divided into three types: free diffusion mixing, turbulent pulsating mixing, and regenerated vortex mixing. Due to the limitation of fixed jet, the methane concentration beyond the jetting region changed little. In addition, the moving jet was used to realize the mixing of methane and oxidizer in wellbore. The sensitivity of different parameters to the distribution of the methane concentration in wellbore was discussed. The results showed that the methane concentration was more sensitive to the wellbore diameter and nozzle diameter. The moving velocity of nozzle was closely related to the distribution uniformity of the methane concentration in wellbore. The moving velocity of nozzle was selected as a single influence parameter to adjust the uniformity of methane distribution in the wellbore, to ensure that methane concentration was within the explosion limit.

1. Introduction

Unconventional oil and gas resources are recognized by the global energy industry as important alternative energy sources. But economic production of these resources requires fracturing stimulation [1]. At present, hydraulic fracturing is the main method to increase the production of unconventional oil and gas resources. However, unconventional oil and gas resources are concentrated in water-deficient areas, and the reservoir clay content is generally high [2, 3]; the process of exploitation by hydraulic fracturing faces the problem of huge consumption of water resources. In addition, clay minerals tend to expand when they meet water and eventually block the gas seepage channel [4]. Recently, the in situ blasting fracturing with formation methane is proposed. The mechanism of this technology is the same as the high-energy gas fracturing. It does not add sand and water. Therefore, it does not need to use special drainage measures after fracturing, and it is useful for environmental protection [5]. However, this technology is still in basic research. There are still many basic problems to be studied. In this paper, we mainly study the mixing characteristics of oxidizers and in situ methane.

Relevant studies showed that under the condition of uniform mixing of methane and oxidizer, the explosion limit range of the mixture of methane oxidizer will be further broadened and the explosion pressure can be further enhanced [6]. In addition, jet feeding can promote the composition to reach molecular level uniformity quickly in the reactor and improve the performance of the reactor [7].

Conventional jet is mainly used for impact cooling, impact crushing, jet combustion, and so on. Gong et al. [8] studied the parameter characteristics of high-speed air jet impacting granular material layer and obtained the influence law of different parameters on the impact capacity of

microporous jet. Cheng et al. [9] established the fracturing flow field of supercritical carbon dioxide jet in the perforated cavity and discussed the influence rule of nozzle pressure drop, nozzle diameter, annulus pressure, and carbon dioxide temperature on the pressure boost effect. In addition, the combustion efficiency can be improved by rapidly mixing fuel and air with jet in the combustion furnace [10]. Lyu et al. [11] simulated the temperature effects of different combustion models on the thermal jet.

Most of the investigations on gas jet mixing were concentrated in chemical industry. Wu et al. [12] studied the influence of momentum ratio and structural parameters on the mixing effect, developed a gas mixer, and realized rapid and efficient mixing of gas. Pei et al. [13] used Fluent software to simulate gas-gas rapid injection mixer in ethylbenzene dehydrogenation unit and studied the mixing effect of rapid injection mixer in ethylbenzene dehydrogenation unit. Sroka and Forne [14, 15] proposed the simplest bend and T-tube mixer. Giorges et al. [16] found that the more nozzles in a mixer, the better the mixing effect would be. To characterize the mixing effect, Devahastin and Mujumdar [17] proposed the standard of mixing index (MI), which symbolized the uniform temperature mixing effect. For the mixing process of fuel and air in a confined space, Liscinsky et al. [18] and Holdeman et al. [19] introduced the index of nonuniformity (Ns) to quantitatively measure the mixing degree of fuel and air.

The methane oxidizer mixing time in the wellbore can be much longer than the gas mixing time in conventional premixed burners. Thus, the mixing mode in this environment is not only jet mixing but also static mixing. In addition, the mixing degree is higher than the jet mixing. In this paper, the air was selected as the oxidizer, to establish the submerged jet mixing model, which could be used to simulate the mixing type of jet in wellbore. The dynamic mesh model was used to simulate the distribution of methane components in the wellbore after air injection in the form of the moving jet. Then, the influence of different parameters on the distribution of methane component in wellbore was researched. The relevant parameters were adjusted according to the rule that the methane distribution in the wellbore was uniform, and the concentration was within the limit of explosion. Moreover, the overall trend was close to the optimal explosion concentration.

2. Horizontal Wellbore Gas Injection Mixing Model

2.1. Geometric Model. As shown in Figure 1, a two-dimensional reference model of the submerged jet flow field in wellbore was established. Before the injection of air, the wellbore was filled with uniformly distributed methane. The flow field is mainly composed of the inner space of nozzle, the annulus between the wellbore and operating tube. The grid of the flow field was divided into three regions by the local meshing method: the encrypted nozzle region with a large variation of the pressure gradient, the encryption region directly affected by the jet flow, and the sparse region. The inlet of the flow field was set as the pressure inlet boundary, and the pressure value was equal to the nozzle inlet pressure. The outlet of the flow field was set as the pressure outlet boundary. The contact boundaries between the nozzle outlet and the flow field in the wellbore and between the encryption and the sparse zones were set as the interfaces. All other boundaries were set as nonslip wall boundaries. The outlet pressure (ambient pressure) and ambient temperature remained constant, and the position of the nozzle changed with time.

2.2. The Governing Equation. The heat transfer was not considered in this paper, so the energy equation was ignored. Since the influence of gravity could be ignored by high-speed jet flow, the simplified mass equation was expressed as [20]

$$\frac{\partial \rho}{\partial t} + \frac{\partial (\rho u_1)}{\partial x} + \frac{\partial (\rho u_2)}{\partial y} + \frac{\partial (\rho u_3)}{\partial z} = S_m, \tag{1}$$

where ρ is the density of fluid, kg/m^3; t represents the flow time, s; u_1, u_2, and u_3 represent the velocity in three directions along the triaxial coordinate system, m/s; and S_m is the mass increase of the continuous phase caused by the discrete phase, kg/(m^3·s).

The momentum equations were as follows [21]:

$$\rho\left(\frac{\partial u_1}{\partial t} + u_1\frac{\partial u_1}{\partial x} + u_2\frac{\partial u_1}{\partial y} + u_3\frac{\partial u_1}{\partial z}\right) = -\frac{\partial p}{\partial x} + \mu\left(\frac{\partial^2 u_1}{\partial x^2} + \frac{\partial^2 u_1}{\partial y^2} + \frac{\partial^2 u_1}{\partial z^2}\right), \tag{2}$$

$$\rho\left(\frac{\partial u_2}{\partial t} + u_1\frac{\partial u_2}{\partial x} + u_2\frac{\partial u_2}{\partial y} + u_3\frac{\partial u_2}{\partial z}\right) = -\frac{\partial p}{\partial y} + \mu\left(\frac{\partial^2 u_2}{\partial x^2} + \frac{\partial^2 u_2}{\partial y^2} + \frac{\partial^2 u_2}{\partial z^2}\right), \tag{3}$$

$$\rho\left(\frac{\partial u_3}{\partial t} + u_1\frac{\partial u_3}{\partial x} + u_2\frac{\partial u_3}{\partial y} + u_3\frac{\partial u_3}{\partial z}\right) = -\frac{\partial p}{\partial z} + \mu\left(\frac{\partial^2 u_3}{\partial x^2} + \frac{\partial^2 u_3}{\partial y^2} + \frac{\partial^2 u_3}{\partial z^2}\right), \tag{4}$$

where ρ is the density of fluid, kg/m^3; P is the fluid pressure, Pa; u_1, u_2, and u_3 represent the velocity in three directions along the triaxial coordinate system, m/s; and μ represents the dynamic viscosity, Pa•s.

State equation:

$$\rho = \frac{p_{\text{op}}}{(R/M_w)T}, \tag{5}$$

where ρ is the density of fluid, kg/m^3; T represents the temperature, K; R is the universal gas constant, mol^{-1}·K^{-1}; M_w represents the molecular weight of the gas; and P_{op} is the operating pressure, Pa.

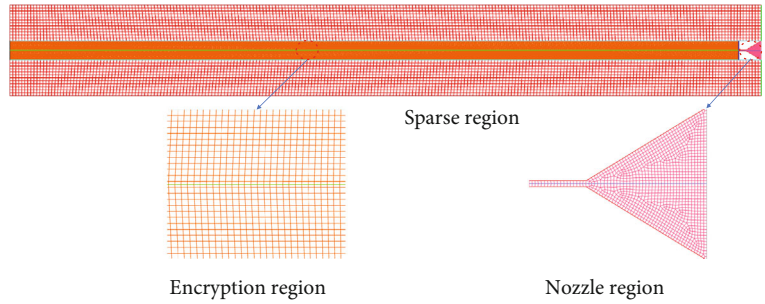

Figure 1: Flow field grid model.

2.3. The Turbulence Model. In 1986, Yakhot and Orszag [22] used renormalization group theory to establish a new turbulence model, the RNG $k-\varepsilon$ turbulence model, in which the coefficients were deduced theoretically and could be used to predict two-dimensional unsteady flow in fluids. Compared with the standard $k-\varepsilon$ model, the RNG $k-\varepsilon$ model contains the bending and rotation flows in the average flow and can better calculate the flow bending (rotation) caused by vortex breakage and attenuation near the jet impacting wall, as well as the flow with high strain rate and large flow bending degree.

The k and ε in the transport equation of the RNG $k-\varepsilon$ turbulence model are defined as follows:

$$\frac{\partial}{\partial t}(\rho k)+\frac{\partial}{\partial x_j}(\rho k u_j)=\frac{\partial}{\partial x_j}\left(\alpha_k \mu_{eff}\frac{\partial k}{\partial x_j}\right)+G_k+G_b-\rho\varepsilon-Y_M+S_k, \tag{6}$$

$$\frac{\partial}{\partial t}(\rho \varepsilon)+\frac{\partial}{\partial x_j}(\rho \varepsilon u_j)=\frac{\partial}{\partial x_j}\left(\alpha_\varepsilon \mu_{eff}\frac{\partial \varepsilon}{\partial x_j}\right)+C_{1\varepsilon}\frac{\varepsilon}{k}(G_k+C_{3\varepsilon}G_b)-C_{2\varepsilon}\rho\frac{\varepsilon^2}{k}-R_\varepsilon+S_\varepsilon, \tag{7}$$

$$R_\varepsilon=\frac{C_\mu \rho \eta^3(1-\eta/\eta_0)}{1+\beta\eta^3}\frac{\varepsilon^2}{k},\quad \eta=S\frac{k}{\varepsilon},\quad S=\sqrt{2S_{ij}S_{ij}},\quad S_{ij}=\frac{1}{2}\left(\frac{\partial u_j}{\partial x_i}+\frac{\partial u_i}{\partial x_j}\right), \tag{8}$$

where k is the turbulent kinetic energy, J; α_k is the inverse effective turbulent Prandtl number of k, dimensionless; G_k is the generation of turbulence kinetic energy due to the mean velocity gradients, kg•J/(m^3•s); G_b represents the generation of turbulence kinetic energy due to buoyancy, kg•J/(m^3•s); Y_M represents the effect of pulsating expansion on the dissipation rate of turbulent kinetic energy in compressible flows, kg•J/(m^3•s); S_k is the user-defined source term, kg•J/(m^3•s); ε is the divergence rate of turbulent kinetic energy, dimensionless; α_ε is the inverse effective turbulent Prandtl number of ε, dimensionless; C_μ, $C_{1\varepsilon}$, $C_{2\varepsilon}$, and $C_{3\varepsilon}$ represent the empirical constant, dimensionless; and S_ε is the user-defined source term, kg•J/(m^3•s).

Table 1 shows the default constants for turbulence models.

Table 1: Default constants for turbulence models.

α_k	α_ε	C_μ	$C_{1\varepsilon}$	$C_{2\varepsilon}$	$C_{3\varepsilon}$	β	η_0
1.393	1.393	0.085	1.42	1.68	0	0.012	4.38

3. Mixing Characteristics of Fixed Air Jet and Methane

The above models were used to simulate the submerged jet flow field of the air injection in horizontal wellbore, as shown in Figure 2. The simulations were performed with the species transport model in FLUENT. The methane-air mixture model existing in the database was selected. In this simulation, to conform to the engineering practice, the diameter of the wellbore was initially selected as 120.6 mm, and the built-in micronozzle was 1 mm in diameter, which was connected to the operating pipe with a diameter of 25.4 mm. The outlet of the flow field was the annular pressure outlet, and the outlet pressure was the ambient pressure. The nozzle inlet was the pressure inlet boundary, which was located on the same section as the outlet. In addition, we set the outlet pressure as 5 MPa and the inlet pressure as 10 MPa to decrease the difficulty of operation on the ground and the amount of methane dilution. The temperature of the fluid had little influence on the strength and range of the jet [23], and the fluid temperature was set to be 330 K, which was consistent with the ambient temperature. When the air passed through the contraction section of the nozzle, the pressure decreased and the speed increased rapidly. It made the collision of gases more violent. After passing through the straight section of the nozzle, it became complete turbulence in a short time. Due to the turbulence pulsation, the air jet beam was mixed with the surrounding static methane, and the surrounding methane would be enfolded by the jet fluid, resulting in entrainment, expansion

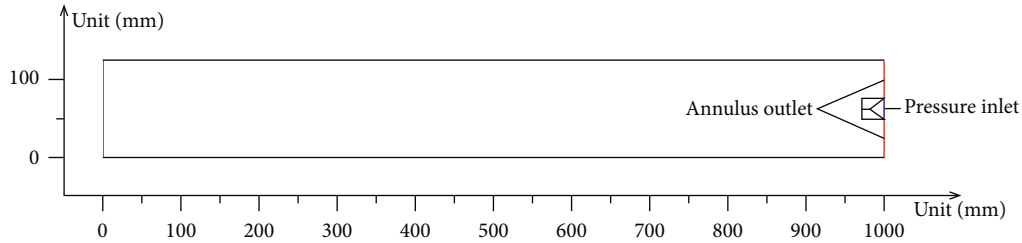

Figure 2: Geometric model.

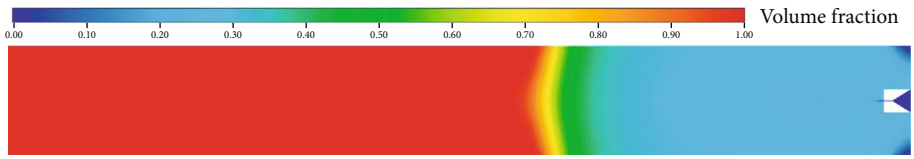

Figure 3: Methane volume fraction in wellbore.

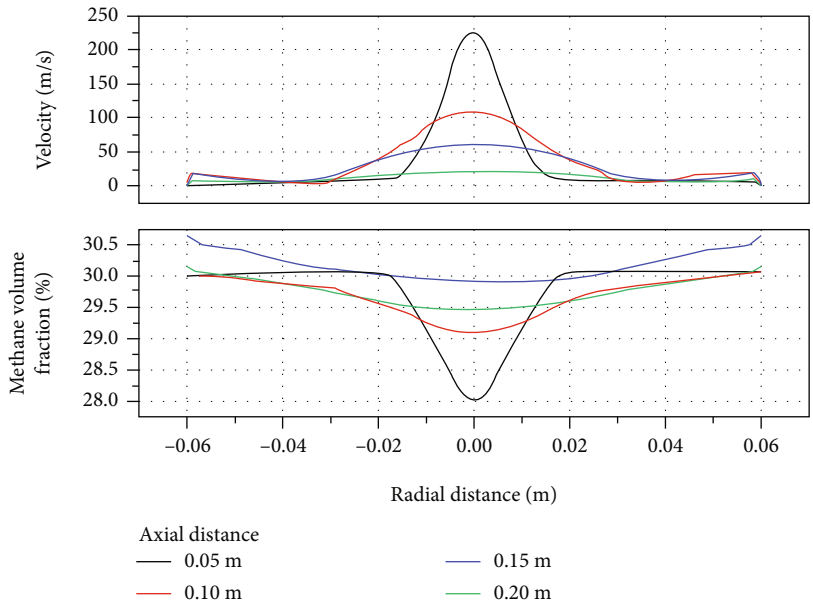

Figure 4: Methane volume fraction and fluid velocity along the radial direction in wellbore.

of the cross-section, and attenuation of the center velocity. It could ensure the gas mixing in the region where the jet passed.

As shown in Figure 3, we conducted a simulation of methane component distribution in wellbore after 1 s of fixed air injection. There was an arc boundary in the middle of wellbore. The methane concentration in the boundary was greatly affected by jet, and it remained unchanged behind the boundary. This boundary was called the jet influence boundary.

To reveal the momentum transformation process in the process of air jet injection, methane concentration and fluid velocity of four observation interfaces close to the nozzle (linear distance from the nozzle is 0.05 m, 0.1 m, 0.15 m, and 0.2 m) within the jet boundary were obtained. As shown in Figure 4, along the axial direction of wellbore, the farther away from the nozzle, the trend of fluid velocity showed flatter. Along the radial direction of wellbore, the farther away from the axis, the velocity was closer to zero. Along the radial direction of wellbore, the methane concentration tended to decrease along both sides of the central axis. However, along the axial direction of wellbore, the farther away from the nozzle, the jet energy was lower. In this case, the degree of substance exchange was lower, and the methane concentration was higher.

Based on the flowing law of fluid, the type of mixing in the wellbore was classified into three categories, as shown in Figure 5. The first region was called free diffusion mixing, which was not affected by the jet. The fluid in this region was mainly methane. After slight disturbance from the outside, the methane molecule occurred diffusion, but the exchange of mass did not occur between methane and air. The second region was called the turbulent pulsating mixing, which was affected directly by the jet. This part was the main section of

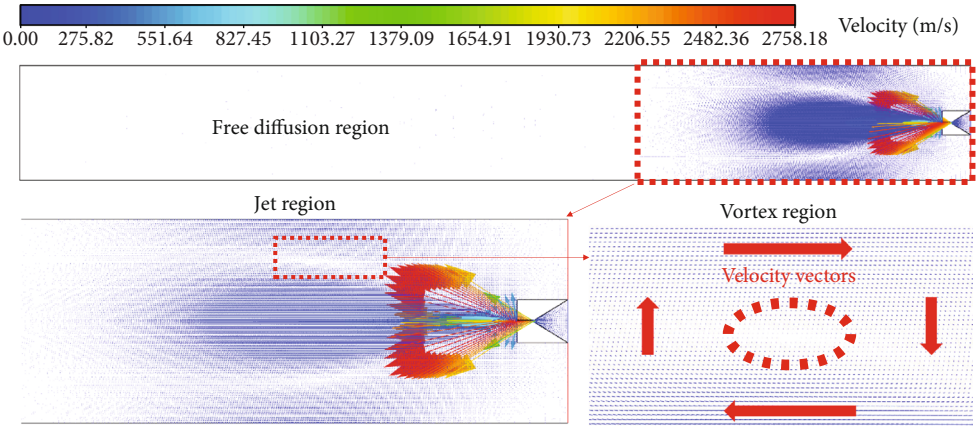

Figure 5: The type of methane-air jet mixing.

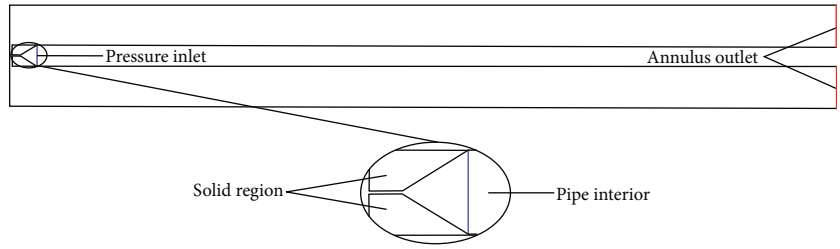

Figure 6: Geometric model of moving jet.

mixing, and its structure was the same as the free jet. The region enveloped by the inner boundary of jet was called the core region of jet, in which the speed remained the initial speed of nozzle exit. In this region, the exchange of species between air and methane and the attenuation of energy did not occur. Thus, this region was completely occupied by air. As the outer boundary expanded, the boundary layer increased and more methane was ensnared. As the jet core region disappeared, the jet structure transformed from the initial part to the main part. In this region, the air and methane collided violently with each other, and the energy and the velocity decreased gradually. The third region was the regenerated vortex mixing, which was different from the general free jet structure. With the expansion of jet boundary, the fluid around the jet structure migrated toward the outlet. The front end of the jet began to vortex under the action of extrusion and entrainment flow, and the growth of the vortex structure and distortion was considered to promote the formation of the methane-air mixture formation process [24]. In this area, the mixture of methane-air was mixed again, and the degree of mixing increased.

4. The Mixing Characteristics of Methane and Moving Air Jet

The limitation of a fixed jet was that the jet distance was limited and the fluid at the far end cannot be fully mixed. To ensure the uniform distribution of mixed combustible and explosive mixture in the wellbore, we carried out a numerical simulation of methane and moving air jet mixing in wellbore. And the influence of wellbore diameter, nozzle diameter, and moving speed of nozzle on the uniformity of methane distribution in wellbore was investigated. As shown in Figure 6, the nozzle was positioned 3 mm away from the vertical wellbore wall and the operating pipe occupied some space in the interior of wellbore during the initial time. As the air injection began, the nozzle moved from the end of the wellbore to the outlet at a special speed and the newly generated encryption region would be occupied with the mixture of air and methane until the mixing was completed in the selected section.

4.1. Wellbore Diameter. To study the law of distribution of methane components in the wellbore with different sizes, the diameters of wellbores were, respectively, set as 50.8 mm, 73 mm, 98.4 mm, and 120.6 mm. As shown in Figure 7, with the increasing of wellbore diameter, the methane concentration in the wellbore increased remarkably, and the dilution degree of methane decreased subsequently. In a small wellbore, the wellbore diameter was lower than the thickness of the jet expansion. In the middle of the jet expansion section, some fluid was vortexed under the action of extrusion and entrainment flow. Because the energy of the middle fluid did not decay more dramatically than the terminal fluid, the velocity of fluid was higher, and the intensity of gas mixing was stronger. However, the control precision for air injection increased with the decreasing of the diameter of wellbore, which would reduce the efficiency of operation. Therefore, an appropriate initial jet velocity and a reasonable diameter of wellbore were conducive to the sufficient mixing of methane and air in wellbore for site

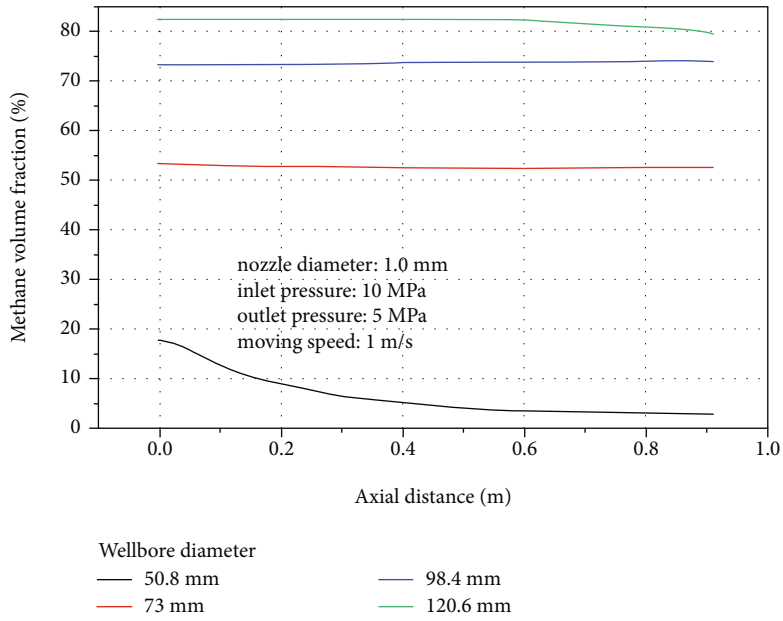

Figure 7: The effect of wellbore diameter on the distribution of methane components in wellbore.

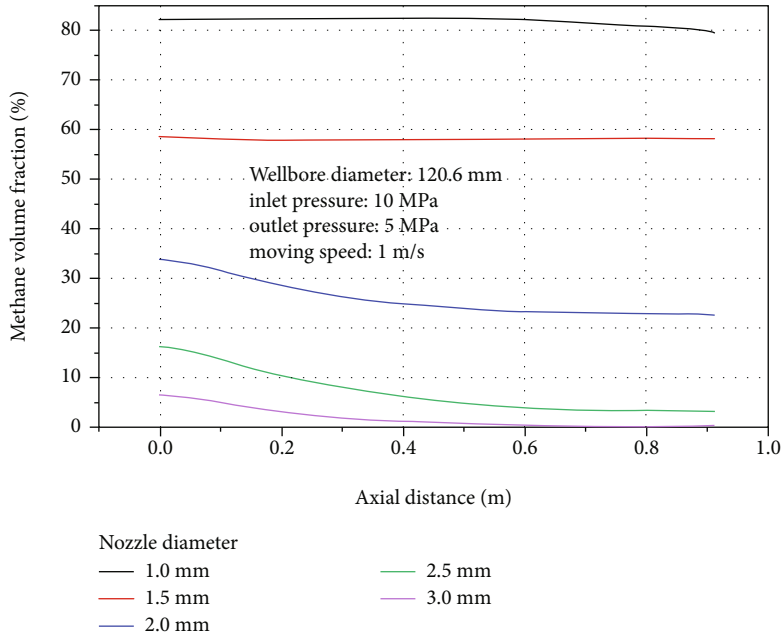

Figure 8: The effect of nozzle diameter on the distribution of methane components in wellbore.

construction, so that the explosion limit of methane was realized.

4.2. Nozzle Diameter. As shown in Figure 8, when the diameter of nozzle increased from 1 mm to 2 mm, the dilution degree of methane increased greatly. As the diameter of the nozzle exceeded a certain size, the dilution degree of methane decreased slowly. As the diameter of the nozzle increased, the diffusion angle and the spreading thickness of jet increased. Consequently, the influence range of jet increased. Thus, the methane concentration in wellbore was easy to be diluted below the lower limit of methane explosion as the air was injected from the larger diameter nozzle. On the contrary, the methane concentration in wellbore was not fully diluted when the air was injected from the smaller diameter nozzle, which was still above the upper limit of explosion. In this case, the conditions of explosion cannot be formed in wellbore. Thus, it could be seen that a nozzle with a small diameter was beneficial to control the methane concentration in wellbore.

4.3. Moving Speed. The air injection in wellbore was a dynamic process. In addition to enlarge the contact area between jet and wellbore, a moving speed of operating tube

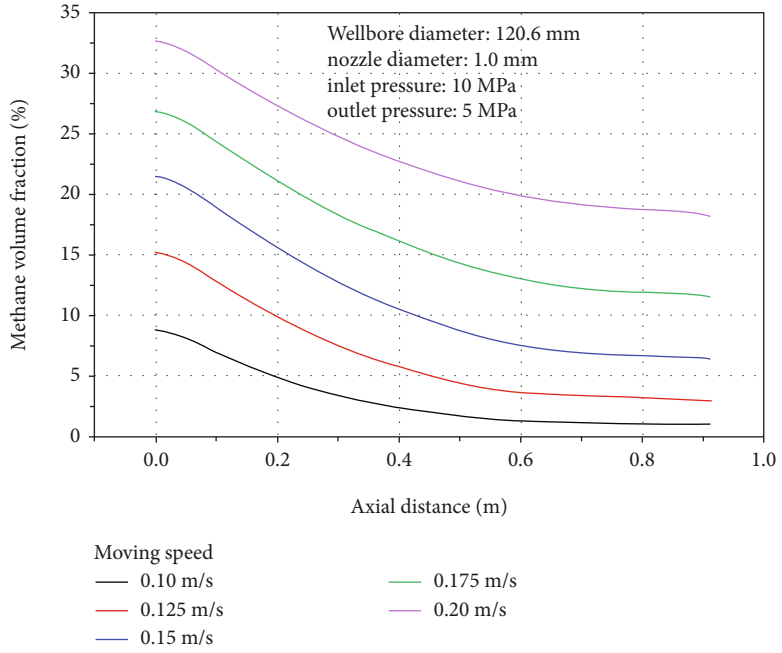

Figure 9: The effect of nozzle moving speed on the distribution of methane components in wellbore.

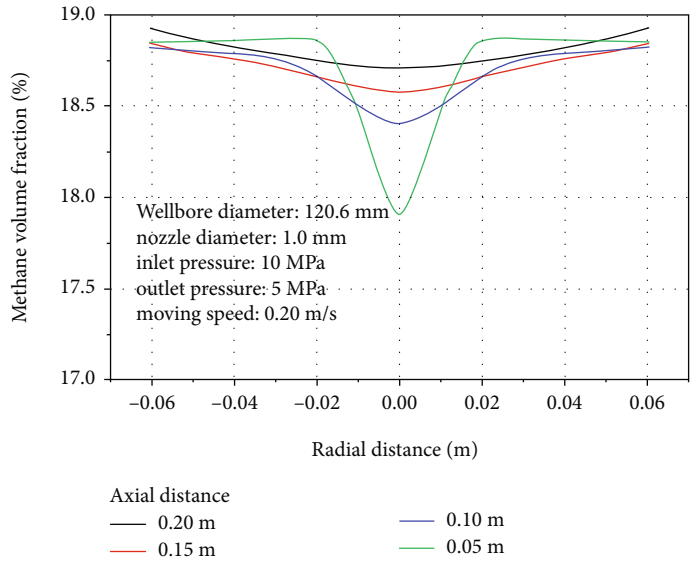

Figure 10: Methane volume fraction along the radial direction in wellbore.

was applied. As shown in Figure 9, the moving speed of nozzle changed the component distribution of methane in wellbore. The higher the moving speed, the more methane remained in wellbore. The jet flow structure varied at different sections of wellbore, although the moving speed of nozzle was kept constant. As a result, the distribution of methane component varied in different axial sections of wellbore after air jet injection. There was an obvious phenomenon of methane accumulation near the vertical wall, and the distribution of methane concentration became more and more uniform as it was far away from the vertical wall. At a certain length along the axial direction, the difference in the methane concentration would be negligible. This was because as the nozzle moved along wellbore, the mixing of methane and air overcame the limitation of jet region. However, the methane concentration was diluted indirectly in the region within the influence limit range of jet. When the air jet passed through the wellbore, the concentration of methane tended to be lower and lower near the outlet.

4.4. Parameter Adjustment. For fixed air jet injection, methane and air could be fully mixed in wellbore, but the uniformity of distribution needed to be improved. Figure 10 shows the trends of the methane concentration in four sections

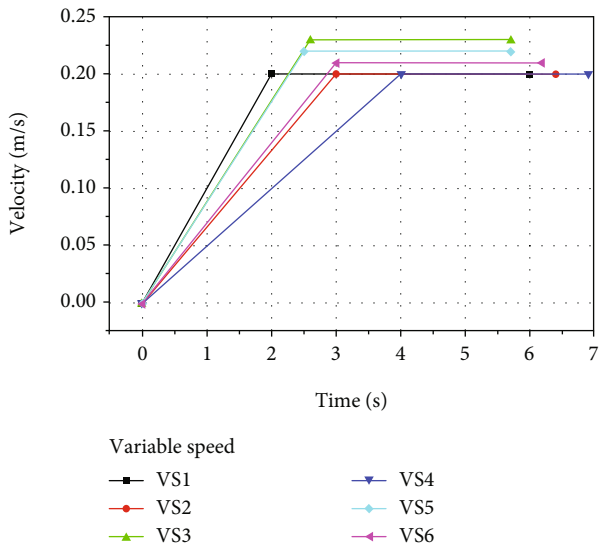

Figure 11: The type of moving speed.

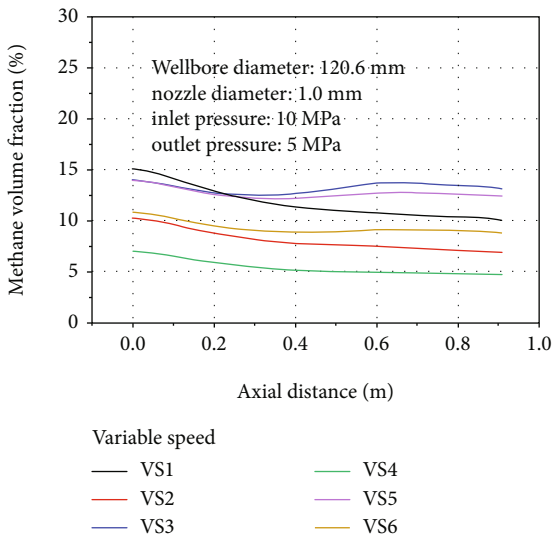

Figure 12: Methane volume fraction at different variable speeds in wellbore.

near the nozzle due to the moving jet. Along the radial direction of the wellbore, the concentration difference of each section was below 1%, and the farther away the section from the nozzle, the smaller the concentration difference. However, along the axial direction, there was an obvious methane concentration area near the wall. With the increasing of the distance to the wall, the methane concentration decreased gradually.

The main purpose of the adjustment was to make the methane concentration in the whole wellbore within the explosion limit, and the methane distribution was uniform as far as possible. In addition, the adjustment would make the methane concentration close to the theoretical optimal explosion concentration. In this case, the stoichiometric methane concentration was 1.07 times [25]. It was known that the explosion limit of methane in the air at room temperature and pressure was 5%~15%, but the wellbore environmental pressure in this paper was 5 MPa and the temperature was 330 K. When the temperature was below 373 K, the influence of temperature on the explosion limit of combustible gas can be ignored [26], and the explosion limit under high pressure can be ensured as follows [27]:

$$\begin{aligned} L_{p1} &= L_1 + 20.6 \times (\lg P + 1), \\ L_{p2} &= L_2 - 0.71 \times (\lg P + 1), \end{aligned} \tag{9}$$

where L_{p1} and L_{p2} are, respectively, the upper and lower limits of explosion of combustible gas under high pressure, %; L_1 and L_2 are, respectively, the upper and lower limits of explosion of combustible gas under atmospheric pressure, %; and P is the initial pressure, MPa.

As the initial nozzle velocity, nozzle diameter, and gas injection time were given, the injection volume of air can be calculated. To ensure that methane in the wellbore was within the limit of explosion (4%-50%), that is, the injection volume of air should be kept between 50% and 96% of the wellbore volume. According to the above results, when the pressure difference between the inlet and outlet was constant, the initial velocity of jet (i.e., the velocity of nozzle outlet) remained constant. The injection time and injection volume at different positions can be controlled by controlling the moving speed of nozzle. The fixed speed of jet was changed to variable speed by adjusting the moving speed of nozzle. In this paper, the moving speed of nozzle was accelerated first and then kept at a constant speed. In this way, the nozzle could stop near the wall for a long time. The injection volume of air was enough to dilute the accumulated methane at the end of wellbore, and the methane concentration in the latter section remained flat. As shown in Figure 11, six different variable speed schemes were tested. The initial speed was 0, and the speed remained constant after accelerating to a certain value until the operating tube was pulled out of the wellbore. As shown in Figure 12, the variable speed of each interval reduced the methane concentration; the difference of the methane concentration along the axial direction in wellbore became smaller. Among them, the sixth scheme worked best, the moving speed increased from 0 to 0.21 m/s in the 3 s, and the distribution of the methane concentration tended to be 10% of the optimal concentration.

5. Conclusion

In this paper, the numerical simulation of methane flow field impacted by air jet in wellbore was carried out by Fluent software, and we drew the following conclusions.

There was a jet influence boundary for air jet injection in the wellbore, and the methane concentration outside the boundary was not affected by the jet.

The mixing types of methane and air jet in wellbore can be divided into three types according to jet structure, one was free diffusion mixing without the direct influence of jet, the other was turbulent pulsation mixing directly

influenced by jet, and the third was vortex mixing formed under the action of extrusion and entrainment flow.

The movement of nozzle was conducive to the mixing of methane and air jet. In this case, the distribution uniformity of combustible and explosive gas in wellbore was improved.

When the fixed jet was used to conduct the mixing of methane and air in wellbore, there was an obvious inhomogeneity of methane distribution along the axial direction of wellbore, and methane accumulated near the vertical wall. As the variable moving speed of nozzle was applied, enough jet time could be ensured near the vertical wall of wellbore, which was beneficial to ensuring the uniformity of methane distribution in wellbore.

Data Availability

The data used to support the findings of this study are available from the corresponding author upon request.

Conflicts of Interest

The authors declare no conflicts of interest.

Authors' Contributions

Chengzheng Cai contributed to the conceptualization. Zhixiang Tao participated in the data curation and reviewed and edited the manuscript; Zengxin Zou participated in the visualization and data curation and was responsible for the software; Yugui Yang participated in writing, reviewing, and editing of the manuscript; Yinrong Feng participated in writing and editing of the manuscript. All authors were responsible for the methodology, software, supervision, and original draft preparation.

Acknowledgments

This research was funded by the National Key R&D Program of China (Grant No. 2020YFA0711800), the Postgraduate Research & Practice Innovation Program of Jiangsu Province (Grant No. KYCX22_2499), and the Graduate Innovation Program of China University of Mining and Technology (Grant No. 2022WLJCRCZL032).

References

[1] T. T. Palisch, M. A. Chapman, and J. Godwin, "Hydraulic fracture design optimization in unconventional reservoirs - a case history," in *SPE Annual Technical Conference and Exhibition*, pp. 1–14, Texas, October, 2012.

[2] X. Jin and S. Shah, "Fracture propagation direction and its application in hydraulic fracturing," *Proceeding of the SPE Hydraulic Fracturing Technology Conference*, 2013, pp. 517–536, Texas, 2013.

[3] W. Y. Jianzhong, W. S. Li, and C. K. Jinliang, "Reservoir characteristics of shale gas in Longmaxi Formation of the Lower Silurian, southern Sichuan," *Acta Petrolei Sinica.*, 2012.

[4] P. Touzel, "Managing environmental and social risks in China," in *Proceeding of International Conference on Health, Safety and Environment in Oil and Gas Exploration and Production*, Perth, Australia, 2012.

[5] D. Zhu and Z. Ning, "High-energy gas fracturing technique to exploit natural gas hydrate reservoir," *Journal of Chongqing University of Science and Technology*, vol. 11, no. 3, pp. 37–39, 2009.

[6] J. I. A. O. Fengyuan, H. U. O. Yujiang, L. I. U. Jinbiao, and Z. H. A. N. G. Huarong, "Experimental study on influence of mixing uniformity onmethane explosion characteristics," *China Safety Science Journal*, vol. 28, no. 8, p. 38, 2018.

[7] W. R. Quinn and J. Militzer, *Experimental and Numerical Study of a Turbulent Free Square Jet*, vol. 31, no. 5, 1988American Institute of Physics, 1988.

[8] S. Gong, F. He, and K. Liu, "Parameter characteristics of using the high-speed air jet to impact granular material layer," *Journal of Mechanical Engineering*, vol. 51, no. 15, pp. 142–147, 2015.

[9] Y. Cheng, G. Li, H. Wang, Z. Shen, S. Tian, and X. Fan, "Pressure boosting effect in perforation cavity during supercritical carbon dioxide jet fracturing," *Atomization & Sprays*, vol. 23, no. 5, pp. 463–474, 2013.

[10] K. Knowles and M. Myszko, "Turbulence measurements in radial wall-jets," *Experimental Thermal and Fluid Science*, vol. 17, no. 1-2, pp. 71–78, 1998.

[11] Z. Lyu, G. Li, X. Song et al., "Comparative numerical analysis and optimization in downhole combustion chamber of thermal spallation drilling," *Applied Thermal Engineering*, vol. 119, pp. 481–489, 2017.

[12] M. Wu, F. Huang, and D. Xu, "Study on gas-gas rapid mixing," *Acta Petrolei Sinica*, vol. 9, no. 2, pp. 112–118, 1993.

[13] K. Pei, R. Li, and Y. Wu, "Numerical simulation on the mixing in a multi-jet gas-gas mixer," *Chemical Reaction Engineering and Technology*, vol. 31, no. 1, pp. 33–39, 2015.

[14] L. Sroka and L. Forney, "Fluid mixing with a pipeline tee: theory and experiment," *AICHE Journal*, vol. 35, no. 3, pp. 406–414, 1989.

[15] L. Sroka and L. Forney, "Fluid mixing in a 90.degree. pipeline elbow," *Industrial & Engineering Chemistry Research*, vol. 28, no. 6, pp. 850–856, 1989.

[16] A. Giorges, L. Forney, and X. Wang, "Numerical study of multi-jet mixing," *Chemical Engineering Research & Design*, vol. 79, no. 5, pp. 515–522, 2001.

[17] S. Devahastin and A. Mujumdar, "A numerical study of flow and mixing characteristics of laminar confined impinging streams," *Chemical Engineering Journal*, vol. 85, no. 2-3, pp. 215–223, 2002.

[18] D. Liscinsky, B. True, and J. Holdeman, "Mixing characteristics of directly opposed rows of jets injected normal to a crossflow in a rectangular duct," in *Proceeding of the 32nd Aerospace Sciences Meeting and Exhibit*, pp. 10–13, Reno, NV, USA, January, 1994.

[19] J. Holdeman, D. Liscinsky, and D. Bain, "Mixing of multiple jets with a confined subsonic crossflow: part II—opposed rows of orifices in rectangular ducts," *Journal of Engineering for Gas Turbines and Power-Transactions of the Asme*, vol. 121, no. 3, pp. 551–562, 1999.

[20] F. Wang, *Computational Fluid Dynamics Analysis: Theory and Application of CFD Software*, Beijing: Tsinghua University Press, 2004.

[21] E. Yuan, *Engineering Fluid Mechanics*, Beijing: Petroleum industry Press, 1986.

[22] V. Yakhot and S. A. Orszag, "Renormalization group analysis of turbulence. I. Basic theory," *Journal of scientific computing*, vol. 1, no. 1, pp. 3–51, 1986.

[23] Y. Cheng, G. Li, H. Wang, Z. Shen, and J. Li, "Impact pressure and parametric sensitivity analysis of supercritical CO_2 jet," *Acta Petrolei Sinica*, vol. 35, no. 4, pp. 765–770, 2014.

[24] J. Yu, V. Vuorinen, H. Hillamo, T. Sarjovaara, O. Kaario, and M. Larmi, "An experimental investigation on the flow structure and mixture formation of low pressure ratio wall-impinging jets by a natural gas injector," *Journal of Natural Gas Science and Engineering*, vol. 9, no. 9, pp. 1–10, 2012.

[25] Fire department of ministry of public security, *Combustible Gas, Steam, Dust Fire Hazard Parameter Manual*, Harbin: Heilongjiang Science and Technology Press, 1990.

[26] L. Zhang, "Analysis of downhole explosion in gas drilling," *Journal of Southwest Petroleum University (Science & Technology Edition)*, vol. 34, no. 5, pp. 146–152, 2012.

[27] S. Hu, *Combustion and Explosion*, Beijing: Beijing Institute of Technology Press, 2015.